frontiers | Frontiers in Earth Science

TYPE Original Research
PUBLISHED 21 February 2024
DOI 10.3389/feart.2024.1287718

OPEN ACCESS

EDITED BY
Binbin Yang,
Xuchang University, China

REVIEWED BY
Lei Gao,
Hohai University, China
Kun Fang,
China University of Geosciences Wuhan, China
Xiaoming Zhao,
Hohai University, China

*CORRESPONDENCE
Changtao Hu,
xj11992023@163.com

†These authors have contributed equally to this work

RECEIVED 02 September 2023
ACCEPTED 23 January 2024
PUBLISHED 21 February 2024

CITATION
Liu J, Pan J, Wang B, Hu C and Liu Q (2024), Study on the shear and deformation characteristics of geogrid-reinforced gravelly soils based on large-scale triaxial tests. *Front. Earth Sci.* 12:1287718. doi: 10.3389/feart.2024.1287718

Study on the shear and deformation characteristics of geogrid-reinforced gravelly soils based on large-scale triaxial tests

Jie Liu[1,2†], Jiadong Pan[1,2†], Bin Wang[1], Changtao Hu[1*] and Qinli Liu[1,2]

[1]Science and Technology R&D Center, Xinjiang Transport Planning Survey and Design Institute Co., Ltd., Urumqi, China, [2]College of Civil Engineering and Architecture, Xinjiang University, Urumqi, China

Geogrid reinforcement has a limiting effect on the lateral deformation and thus improves the shear strength of the soil, the overall strength of the soil and the overall stability of the corresponding geotechnical structure. In this study, large-scale triaxial tests without and with geogrid reinforcement were conducted on three typical gravelly soils in Xinjiang using a large-scale triaxial apparatus. The shear strength and deformation characteristics of gravelly soils with different particle shapes and the stress-strain relations, strength characteristics, damage patterns, and reinforcement effects of gravelly soils with and without reinforcement were investigated. Geogrid reinforcement effectively enhances the strength of the soil; the internal friction angle remained relatively constant with and without reinforcement, whereas the cohesive force increased significantly. The reinforcement effects interpreted from the results obtained from the triaxial tests were discovered when a certain deformation or relative displacement with the reinforcement materials of the soil occurred. Under uniform test conditions, the volumetric strain of the samples of gravelly soil with reinforcement significantly decreased with increasing confining pressure, and the difference in volumetric strains with and without reinforcement was greater when the confining pressure was higher. The highlight of this study is its significance in explaining the reinforcement mechanism in gravelly soils and in selecting engineering design parameters.

KEYWORDS

geogrid reinforcement, large-scale triaxial test, shear behavior, coarse-grained soil, reinforcement coefficient

1 Introduction

Gravelly soils are widely distributed in the Gobi Desert, mountains, and rivers of northwest China; they are a kind of coarse-grained soil and a typical granular material. Gravelly soils include more than 50% gravel or mixes of cohesive soils with numerous coarse particles and may be categorized as angular, round, or sandy gravelly soils based on their particle gradation and shape. Soils with excellent and good engineering characteristics have a high degree of compaction and shear strength, good permeability, low settlement deformation, and less occurrence of earthquake-induced liquefaction. It was found that gravelly soils have stronger compressive and shear strengths compared to clays, but their tensile strengths decrease significantly with increasing gravel content (Zhang et al., 2022).

Reinforced soil refers to the laying of geosynthetics in the soil and is an effective means of improving soil properties. Yu et al. (2019) conducted triaxial tests on geogrid-reinforced soil and discovered that geogrid reinforcement reduced settlement compared to unreinforced soil in the case of a train running at high speed. Asakereh et al. (2013) ran 5000 cyclic loading tests on footings constructed on unreinforced and geogrid-reinforced sand with circular voids subjected to a combination of repeated loads and found that the addition of geogrid reinforcement could reduce settlement. Gu et al. (2016) established a finite element model to simulate a geogrid-reinforced flexible pavement structure and analyzed the geogrid-reinforced and unreinforced pavement models separately. The results showed that geogrid reinforcement can effectively reduce rutting damage in pavement and subgrade. With a large-scale direct shear device, Wang et al. (2014) tested the shear strength of geogrid-reinforced sandy soils. To measure the horizontal and vertical deformation ratios of triaxial test soil samples during deformation based on consolidated undrained triaxial testing, Liu and Chen (2011) employed digital image processing methods. The analysis of the aforementioned two results shows that although the geogrid significantly limits the transverse deformation of medium-grained sandy soil, it ultimately is unable to avoid failure of the composite reinforced soil. The study mentioned above demonstrates that when employing gravelly soils as roadbeds exposed to traffic loads, the application of geogrid reinforcement may improve the mechanical properties of the soil.

Studies on the strength and deformation characteristics of composite reinforced soil using triaxial tests have primarily focused on fine-grained soils. Estabragh et al. (2011) and Liu and Chen (2011) conducted large-scale triaxial tests on nylon fiber- and flax fiber-reinforced clays, respectively. Their results and those of many other researchers, such as Tong et al. (2019) et al., show that the shear strength of clay with fibers increases with increasing fiber content and that the cohesion and internal friction angle of the clay increase with reinforcement. According to Qu and Sun (2016) and Ruan et al. (2020), cohesive soils reinforced with fiber exhibit less expansibility as the fiber concentration increases. Yang et al. (2023) proved that when the mass per unit area of the geotextile increased, the interface friction between the soil and geotextile increased, and the cracking of the soil was effectively inhibited. Liu and Cai (2009) used the finite element method to compare the dynamic response of pavements without or with geogrid reinforcement and concluded that geogrid reinforcement can provide lateral restraint to the subgrade by increasing the interfacial shear resistance performance and can improve the stress distribution in the subgrade layer; thus, geogrid reinforcement also reduces surface deformation and uneven settlement. Mittal and Shrivastava (2020) provided a model with a confidence level greater than 95% to predict the settling of landfill clay cover barriers reinforced with geogrids using the findings from triaxial tests to compute the soil's elastic modulus. Numerous researchers at home and abroad have carried out triaxial tests on various reinforced soils. Although the test outcomes vary, all of them show that reinforcement has a limiting and improving effect on the lateral deformation and shear strength of the soil. They also demonstrate that triaxial tests on reinforced soil are an efficient way to obtain exact stress–strain characteristics and strength properties of composite reinforced soils.

Many studies have experimentally found that the tensile strength of coarse-grained soils is related to their gravel content. Zhang et al. (2022) conducted tensile tests on coarse-grained soils with different gravel contents. Chen et al. (2018) conducted direct shear tests on geogrid-reinforced soils with different gravel contents, and both of these studies showed that the tensile strength of the soil decreased obviously with increasing gravel content. However, Chen et al. (2018) discovered that geogrids significantly inhibited soil expansion and enhanced the soil's tensile strength. From their study, it was found that when geosynthetic materials with mesh structures, such as geogrids, are used to reinforce loose gravelly soils, the high compressive capacity of the soil and the high tensile capacity of the reinforcement materials can be fully utilized, and the interlocking action between the reinforcement and soil can ensure that the reinforcement effect is fully exploited. However, much of the research on triaxial tests of reinforced coarse-grained soils has been done on sandy soils, and only a few researchers have tested reinforced gravelly soil. Triaxial tests were first used by Koga et al. (1988) to explore reinforced sandy soils using metal strips as the reinforcement material. Skuodis et al. (2020) conducted triaxial tests on sandy soils reinforced with flexible geogrids or rigid geogrids and unreinforced sandy soils. By comparing the test results, it was found that the reinforcement behavior increased the internal friction angle and cohesion of the sandy soil, thus increasing the shear strength of the soil. Ye and Fu (2018) conducted triaxial tests on reinforced mudstone with bamboo material, and their results also found that the increased shear capacity of the composite reinforced soil could inhibit the sliding shear failure of the filled embankment. Sarkar and Hegde (2022) chose geogrids to reinforce sand, steel slag, and construction and demolition waste (CDW). These materials were tested in triaxial tests, and the results revealed that the geogrid reinforcement enhanced the shear strength of the backfill material. The strong cohesiveness that the geogrid imparted to the fill material was the cause of the increase in shear strength, while the internal friction angle changed only slightly. Additionally, the nonlinear stress–strain behavior of the geogrid-reinforced waste material was approximated by the Duncan–Chang hyperbolic model.

In summary, reinforcement is an effective means to improve the engineering characteristics of soils, especially those with a low cohesion. Numerous studies have investigated the shear strengths of and stress–strain relationships between coarse-grained soils and geogrid-reinforced sandy soils, but the complexity of the engineering properties of gravelly soils leads to a more complex reinforcement mechanism than that of fine-grained soils. There are currently only a few studies on the geogrid reinforcement mechanism of gravelly soils and the deformation and strength properties of composite reinforced soil in Xinjiang, which affects the promotion of reinforced structures in this region. In this study, a series of large-scale triaxial tests were conducted to compare and analyze the shear strengths, deformation characteristics, and internal friction angles of gravelly soils with different particle shapes, as well as the stress–strain relations, strength characteristics, failure morphology, and reinforcement effects of gravelly soils with and without reinforcement. The results of this study are important for explaining the reinforcing mechanism of gravelly soils and the selection of engineering design parameters.

TABLE 1 Three-phase ratio index for three gravelly soils.

Samples type	Sample no.	Maximum dry density (g/cm^2)	Optimum water content (%)	Maximum dry density at 92% compaction (g/cm^2)
Round gravelly soil	S1	2.28	4.6	2.10
Angular gravelly soil	S2	2.25	5.6	2.07
Sandy soil	S3	2.23	6.8	2.05

FIGURE 1
Soil sampling location. **(A)** Round gravelly soil. **(B)** Angular gravelly soil. **(C)** Sandy soil.

2 Materials and methods

2.1 Materials

The soils for this test, which are round gravelly soil, angular gravelly soil, and sandy soil, were taken from three different regions in Xinjiang and have the following properties. The three-phase ratio indexes of the three gravelly soils are shown in Table 1.

The round gravelly soil (S1) in Figure 1A was taken from Shawan County, Tarbagatay Prefecture, Xinjiang, and is a sandy gravel layer made of alluvium and sediment; it is a widely used roadbed filler for Xinjiang mountain roads. The round gravelly soil particles are mostly gray, medium dense, slightly water-wet, subcircular, and well sorted, the parent rock is mainly sandstone, the filler is medium and coarse sand, the particles are mostly subcircular, and the soil strength is high.

The angular gravelly soil (S2) in Figure 1B was taken from Aketao County, Kizilsu Kirgiz Autonomous Prefecture, Xinjiang, from a mudflow-formed accumulation; this soil is poorly graded gravel with a granitic parent rock, caesious to gray-cyan in color, and typical angular gravelly soil.

Sandy soil (S3) in Figure 1C was taken from Hami, Xinjiang. The site is located in the pre-mountain alluvial plain, in the intermountain basin of Wutongwozi spring, the low mountainous area and pre-mountain micro-hilly area of the Karlik Mountains, and the intermountain basin area of Yiwu-Xiama cliff, and the geomorphology is residual-colluvial low-mountain hills and diluvial plains. The soil color is mainly khaki-grayish yellow, and the parent rock is mainly sandy soil with sandstone and siliceous rock.

The geogrid used in the test was a biaxial geogrid made of polypropylene composites with the specification of TGSG15-15: a mesh net spacing of 37 mm × 40 mm, longitudinal rib width of 4 mm, transverse rib width of 5 mm, and thickness of 2.4 mm. The tensile strength and tensile stiffness indexes of the geogrid were measured by tensile tests, as shown in Table 2. In the test preparation stage, the geogrid was cut into circular samples with a diameter of 29.5 cm, as shown in Figure 2.

2.2 Sample preparation

Zekkos et al. (2008) and Zekkos et al. (2012) have shown that the coarse particles in the soil sample will produce noticeable scale effects if the samples are used directly for the tests. Therefore, they suggested that the maximum particle size in the test material should be less than 1/6 or even 1/10 of the specimen diameter to avoid excessive scale effects as much as possible. Because of the limitation of the instrument size, the specimen diameter D=300 mm and height H=600 mm were used in this experiment. To ensure that the test results were not affected by the scale effect of the test materials, gravelly soil with particle sizes larger than 60 mm was removed. The maximum particle size of the test materials was controlled below 1/5 of the specimen diameter, i.e., the maximum allowable particle size was 60 mm, and the scale effect could be ignored in this case (Qingguo, 1999). The oversized particle content was replaced by the equal mass substitution method, in which the allowable coarse particle materials (from 5 mm to the maximum allowable particle size) were substituted for the oversized particles in equal proportions (Hai-tao and Xiao-hui, 2009; Tang et al., 2014;

TABLE 2 TGSG30-30 bidirectional geogrid mechanical indicators.

Parameters	Tension at failure (kN/m)		Strain at failure (%)		Tension at 2% strain (kN/m)		Tension at 5% strain (kN/m)	
Direction	Vertical	Horizontal	Vertical	Horizontal	Vertical	Horizontal	Vertical	Horizontal
Values	30.7	27.0	27.6	19.8	5.7	6.7	11.0	11.7

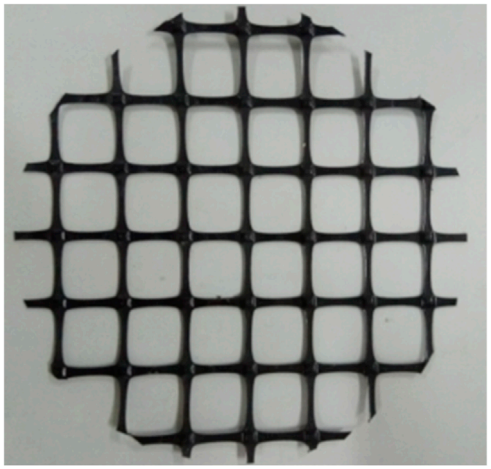

FIGURE 2
The geogrids samples used in experiments.

Yong-zhen et al., 2015), which can maintain the framework role of the coarse grains and the continuity of the coarse grain composition to more closely mimic the behavior of a natural grain composition. Figure 3 depicts the grain composition of the three gravelly soils utilized in the small-scale tests. It can be seen from the grading curve that the grading curve of S3 is steep, which is poor grading soil. The curves of S1 and S2 are relatively flat, and the soil samples have good gradation.

First, a large Proctor compaction test was used to determine the maximum dry density and optimum water content of the three soil samples. Then, after mixing the test materials well, according to the test design plan, a layer of cut geogrid was laid horizontally at different parts of the specimens and compacted in layers to shape a reinforced composite. Finally, when the specimen at the reinforced layer was compacted, the surface was roughened to ensure that the interlocking and frictional characteristics of the reinforced soil could be effectively developed. Under the condition of 92% compaction, the working conditions were divided into 4 types depending on the reinforcement: no reinforcement, 1-layer reinforcement, 2-layer reinforcement and 3-layer reinforcement, and the geogrid under every working condition was reinforced with equal spacing, as shown in Figure 4. The preparation process of the large-scale triaxial test sample is shown in Figure 5.

The test was conducted in the dynamic and static triaxial laboratory of the Institute of Rock and Soil Mechanics with a TAJ-2000 large dynamic and static triaxial instrument. As the Xinjiang region has an arid and semiarid climate, the permeability of this gravelly soil is good, and the pore water pressure dissipates quickly during the construction process, causing the roadbed to remain unsaturated under normal working conditions. However, when the construction speed is too fast, during heavy rainfall-type floods in summer, or under other special circumstances, the pore water pressure dissipates slowly in the roadbed soil, which will be briefly saturated. The experimentation in this work is based on the actual situation of roadbed work in the Xinjiang region, considering two working conditions of the soil, namely, the saturated state and unsaturated state.

A total of 8 groups of large-scale triaxial shear tests were conducted. Consolidated drained (CD) shear tests were conducted in 6 groups, all with unsaturated conditions, mainly to study the deformation characteristics and model parameters of soil S1 and its 3 reinforced composites with different reinforcement layers and reinforcement spacing, soil S2 and soil S3. Two groups of consolidated undrained (CU) shear tests, both in the saturated state, were conducted with the main purpose of comparing the stress–strain relations, strength characteristics, failure morphologies and reinforcement effects of round gravelly soil test materials with and without reinforcement in saturated and unsaturated states. The test program is shown in Table 3.

Gravel soil large triaxial test soil particles, instrument size, if one sample is compacted in a single stage of confining pressure, the soil usage is high, and the cost is high. Furthermore, the regularity of the test results is poor due to the discreteness of gravelly soils (Huachen, 2004). The multistage confining pressure test method for one sample can not only save operation time but also avoid the poor regularity of results due to the differences between the samples. This method has been written into the relevant specifications and is widely used in engineering practice (Guo, 2003; Huachen, 2004). In this test, the multistage confining pressure test method of one sample was used in accordance with the Test Methods of Soils for Highway Engineering.

2.3 Test procedure

For CU tests, the samples are first saturated by pumping out the air after the installation was completed, and the saturation time was more than 20 h. Then, the deaerated water was pressed into the soil sample, and when the pore water pressure was raised to a certain level, the incoming and outgoing water volumes were equal. Applying confining pressure for consolidated drainage, the amount of consolidated drainage was measured at the same time with a controlled accuracy of 0.1 mL until the amount of drainage stabilized (Wang-Guo et al., 2010). Until the residual air in the soil sample is dissolved in water under pressure, the saturation of the soil sample is complete.

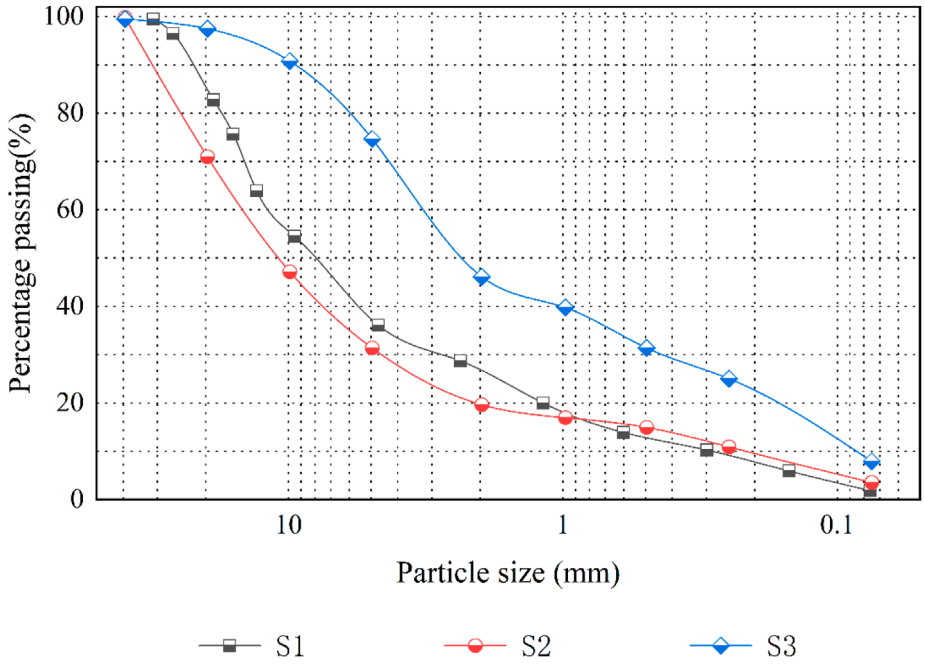

FIGURE 3
The grading curves of the filler.

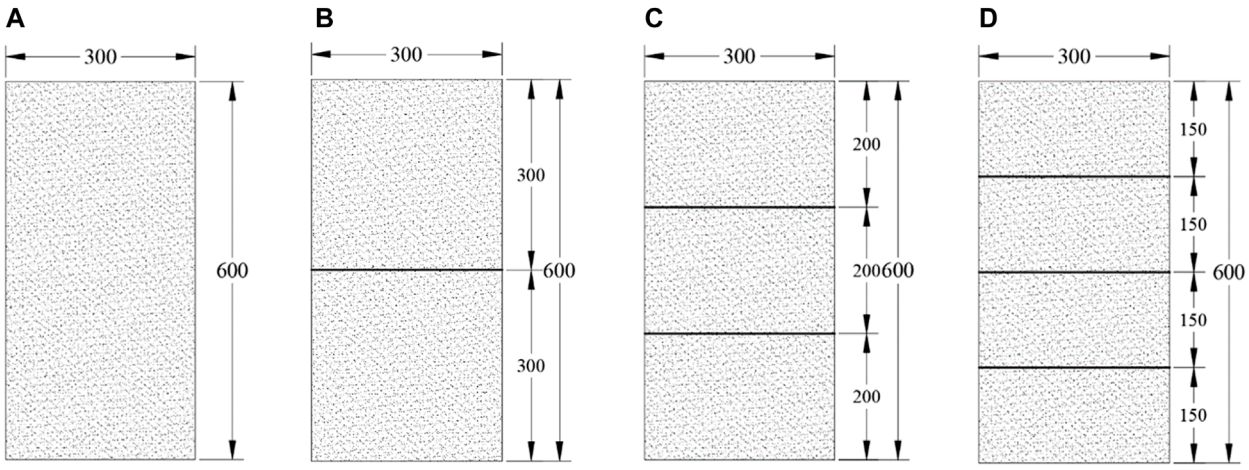

FIGURE 4
The layout of the geogrids for large-scale triaxial testing (mm). **(A)** No reinforcement: **(B)** 1-layer reinforcement, **(C)** 2-layer reinforcement, and **(D)** 3-layer reinforcement.

The test was isotropically consolidated, and the drainage valve was opened to drain (Chen et al., 2014). The confining pressure was adjusted to a predetermined value and kept constant to allow the sample to sufficiently consolidate. During the consolidation process, the volume change readings and the pore water pressure of the sample were recorded, and the consolidation process was considered complete when the readings were stable and the pore water pressure was within the specified range.

In this test, four levels of 200, 400, 600, and 800 kPa confining pressure were applied to the same sample in a graded manner from small to large. Axial pressure was added to shear the sample under the effect of the first level of confining pressure, and loading was stopped when the axial pressure no longer increased or the stress difference between two adjacent levels was less than 5 kPa. Then, the second level of confining pressure was applied immediately. After stabilizing for 10 min, axial pressure was applied to shear the sample, and loading was stopped again when the axial pressure no longer increased or the stress difference between the two adjacent levels was less than 5 kPa. Therefore, shear testing was continued at the third and fourth levels under the action of the confining pressure

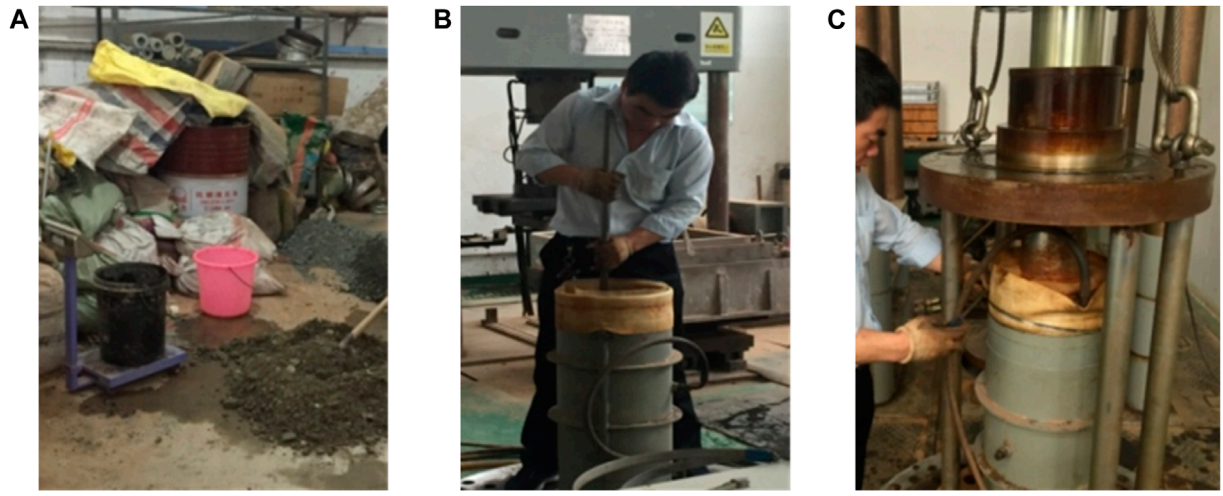

FIGURE 5
The preparation process of a large-scale triaxial test sample. **(A)** Preparation of filler materials. **(B)** Compaction in layers. **(C)** Installation of specimen.

TABLE 3 Test program of the large-scale triaxial testing of reinforced soil.

No.	Conditions	Sample no.	Reinforcement layers	Reinforcement spacing (cm)	Method	State	Dry density (g/cm^3)	Water content (%)
1	Condition1	S1	—	—	CD	unsaturated	2.10	6.6
2	Condition2	S1	1	30	CD	unsaturated	2.10	6.6
3	Condition3	S1	2	20	CD	unsaturated	2.10	6.6
4	Condition4	S1	3	15	CD	unsaturated	2.10	6.6
5	Condition5	S1	—	—	CU	saturated	2.10	—
6	Condition6	S1	2	20	CU	saturated	2.10	—
7	Condition7	S2	—	—	CD	unsaturated	2.07	7.6
8	Condition8	S3	—	—	CD	unsaturated	2.07	7.6

until the sample experienced shear failure. If the principal stress differential did not peak, the principal stress differential at 15% of the axial strain was taken as the principal stress differential at failure (Berre, 1986).

3 Results and analysis

3.1 Analysis of the stress-strain relationship

The CD triaxial shear test was conducted on the unreinforced gravelly soils and reinforced gravelly soils (with the addition of 1–3 layers of geogrid) under continuously applied confining pressure conditions. The test was stopped after the sample reached 15% axial strain, and the molds were disassembled at the end of the test. The sample was found to show significant bulging damage (Ai et al., 2021), but no surface fracture was evident. The reinforcement materials were intact, and no fracture occurred in the ribs, but obvious scuff marks appeared on the surface of the reinforcement materials, and the damage between the materials and the soil was mainly frictional damage. The curves of the relationship between the principal stress differential and axial strain from condition 1 to condition 4 are shown in Figure 6.

As the confining pressure increases, the amount of particle crushing also gradually increases, and the position of the particles rearranges, making the sample more compact (Jia-ming et al., 2009): The interlocking action between the geogrid and the soil becomes more powerful. With increasing axial stress, the strain of the geogrid-gravelly soil composite increased continuously and showed obvious strain-hardening behavior (Zhang et al., 2020). However, the increment of deviator stress in condition 1 during

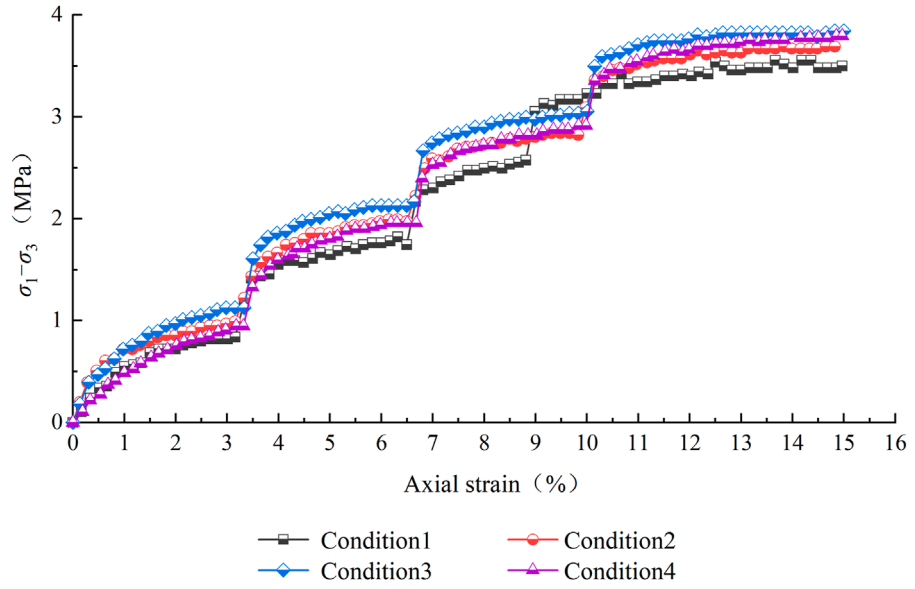

FIGURE 6
Curves of the relationship of $(\sigma_1-\sigma_3)-\varepsilon_1$.

each loading stage was smaller than that in the other three reinforced groups.

To analyze the change process of the principal stress difference during the vertical stress application in the triaxial test of reinforced soil, during each level of isotropic consolidation, the soil body is in isotropic compression during isotropic consolidation, while the geogrid in the soil body is also in compression in the axial direction. At the beginning of the vertical stress application, the axial strain of the triaxial sample was small, the geogrid did not play a role, and the unreinforced soil and the reinforced composite stress-strain curves were basically the same initially. However, with increasing load, the soil deformation gradually increases, and the mutual movement between soil particles makes the soil particles rearrange. Because of the interlocking action between the geogrid and soil particles and because the elastic modulus of the soil is much larger than the elastic modulus of the geogrid, the soil was gradually subjected to an outward tensile force from the center of the sample. When the lateral deformation of the sample returned to the state before the application of the confining pressure, the lateral restraint effect of the geogrid on the rearrangement of soil particles was gradually produced. With increasing axial displacement, this lateral restraint effect was gradually enhanced, and the role of the geogrid became increasingly important. The stress-strain curves of the reinforced composites gradually became higher than that of the unreinforced gravelly soil, and the deviator stress and peak strength at yield of the reinforced samples increased to different degrees compared with those of the unreinforced soil.

3.2 Strength characteristics analysis based on Mohr-Coulomb theory

The Mohr circles and Mohr-Coulomb strength envelopes for three typical gravelly soils and reinforced gravelly soils in the Xinjiang region under different confining pressures are shown in Figure 7.

Table 4 shows that the cohesive force *c* is not zero for the three unreinforced gravelly soils in the unsaturated condition, indicating that it is obviously conservative to take zero for the cohesive force of soils in the arid and less rainy areas.

Comparing working conditions 1 and 5, we can find that the friction angle φ is not much different between the saturated and unsaturated conditions, but the cohesion *c* is larger in the unsaturated condition than in the saturated condition; because the samples for the unsaturated tests are formed by layering under the optimum water content, and the soil in the model is composed of solid particles, water, and gas, mutual adhesion and embedment of the soil particles occur. After the saturation process, the samples are in a saturated state, the spaces between the soil particles are filled with water, and some of the small particles are even in suspension, so that the friction coefficient of the soil particles decreases and the cohesion c decreases, even to zero.

Comparing conditions 3 and 6, it can be found that the friction angle φ is not much different between unsaturated and saturated conditions for specimen S1 with reinforced soil. However, the cohesion *c* is larger in the saturated condition than in the unsaturated condition, which is the opposite of the test result of unreinforced gravelly soil. The reason for this is that in the saturated state, there is water adhering to the surface of the soil particles, and the soil particles are filled with free water between them, so the soil particles move more easily than in the unsaturated state, and the samples are more likely to develop small deformations. Since reinforced soil is a typical composite material, the outward expansion and deformation of the samples under vertical loading produces an inward binding force on the soil, which itself is subjected to outward tension, and the reinforced composite shows a certain cohesion *c*. The cohesion exhibited by gravelly soils in the unsaturated state is due to only the cohesion of some of the clay in the soil and the embeddedness and

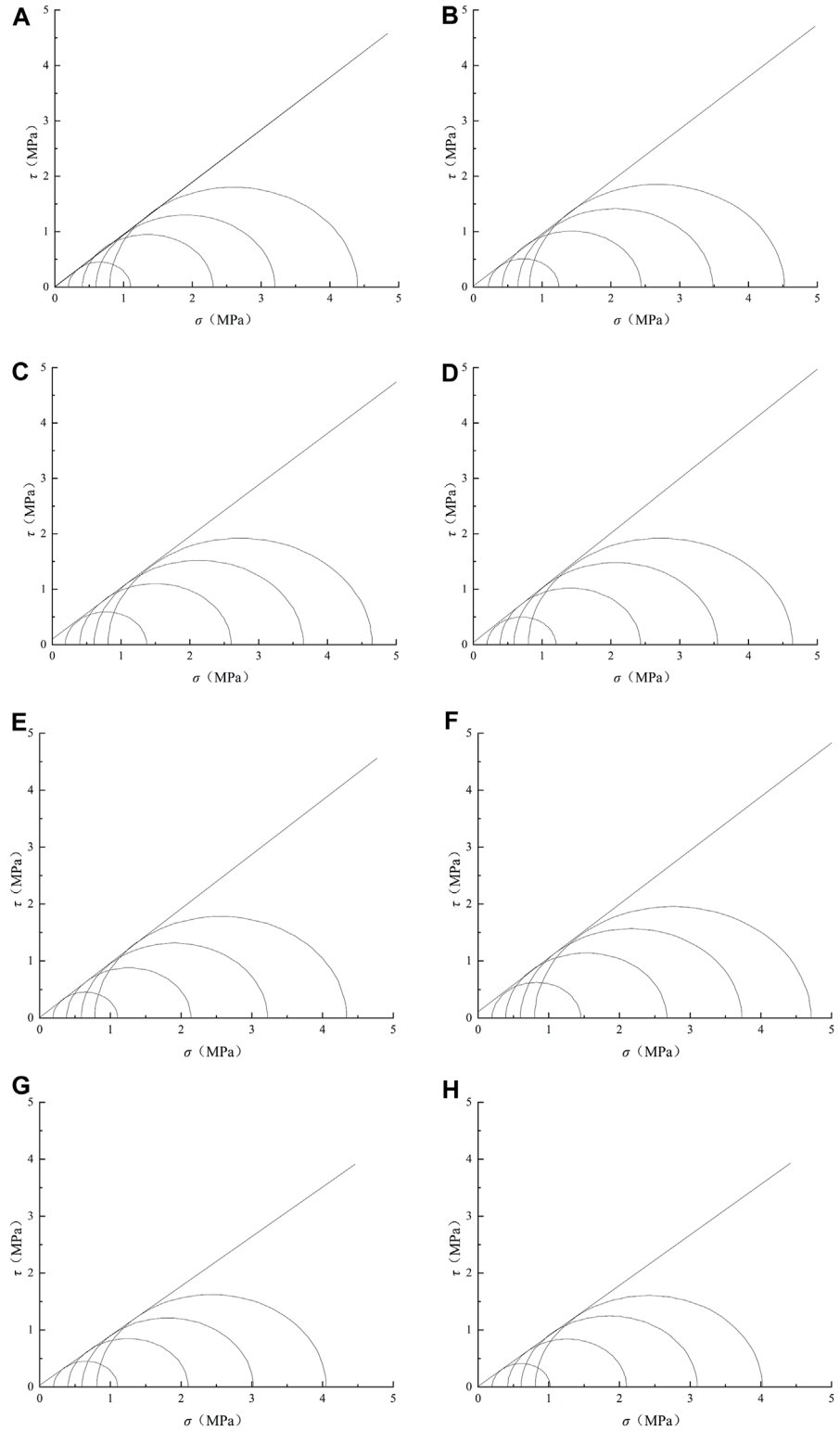

FIGURE 7
Mohr envelopes of gravelly soil samples. **(A)** Condition 1. **(B)** Condition 2. **(C)** Condition 3. **(D)** Condition 4. **(E)** Condition 5. **(F)** Condition 6. **(G)** Condition 7. **(H)** Condition 8.

TABLE 4 Triaxial test gravelly soil and reinforced gravelly soil shear strength index.

No.	Conditions	Sample no.	Reinforcement layers	Reinforcement spacing (cm)	Method	State	c (MPa)	φ (°)
1	Condition1	S1	—	—	CU	unsaturated	0.006	43.38
2	Condition2	S1	1	30	CU	unsaturated	0.038	43.64
3	Condition3	S1	2	20	CU	unsaturated	0.070	43.62
4	Condition4	S1	3	15	CU	unsaturated	0.021	44.55
5	Condition5	S1	—	—	CD	saturated	0	43.80
6	Condition6	S1	2	20	CD	saturated	0.087	43.70
7	Condition7	S2	—	—	CU	unsaturated	0.018	41.52
8	Condition8	S3	—	—	CU	unsaturated	0.012	41.70

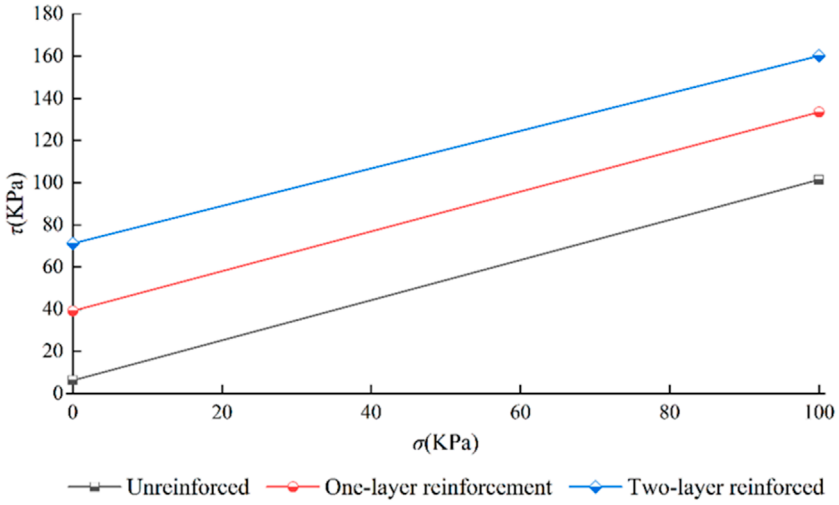

FIGURE 8
Curves of the relationship of σ−τ with different reinforcement layers of gravelly soil.

cohesion between the soil particles. Therefore, the cohesion in the saturated state is larger than that in the unsaturated state.

Figure 8 depicts the σ-τ curves for gravelly soils with various reinforcement layers. It can be seen from Figure 8 that the Mohr-Coulomb strength envelopes from conditions 1 to 3 are almost parallel, indicating that the internal friction angle φ of gravelly soils does not change significantly with and without reinforcement and that the effect of reinforcement on the φ value of gravelly soils is small enough that it is considered to be basically unchanged. The strength line of the reinforced gravelly soil does not pass the intercept point of the unreinforced soil and increases, i.e., the c value of the reinforced gravelly soil is greater than that of the unreinforced gravelly soil. The c value increases with the reduction in the reinforced layer spacing, which means that the increase in the strength of the geogrid-reinforced soil is mainly due to the increase in the cohesion c of the soil. The geogrid is in a state of tension in the soil, and a tangential force is generated at the reinforcement-soil interface and restrains the lateral expansion deformation of the soil. This tangential force results in the side of the sample being subjected to $\Delta\sigma_3$ with the same direction and effect and the same distribution as σ_3 while being subjected to the confining pressure σ_3. As the number of reinforced layers increases, the value of $\Delta\sigma_3$ increases, and then the value of σ_1 required for soil failure increases; thus, the shear strength of the reinforced soil is improved (Shengyou, 2006).

The above analysis shows that the geogrid-gravelly soil composite with geogrids with an elastic modulus much larger than that of the gravelly soil generates an inward frictional resistance between the reinforced soil and increases the perimeter pressure, which effectively improves the strength of the soil. The geogrid-reinforced gravelly soils conform to Mohr-Coulomb shear strength theory, and it is reasonable to explain the reinforcement mechanism by pseudo-cohesion theory. The tests are in general agreement with the experimental results of many other studies (Yi, 2011; Du et al., 2022).

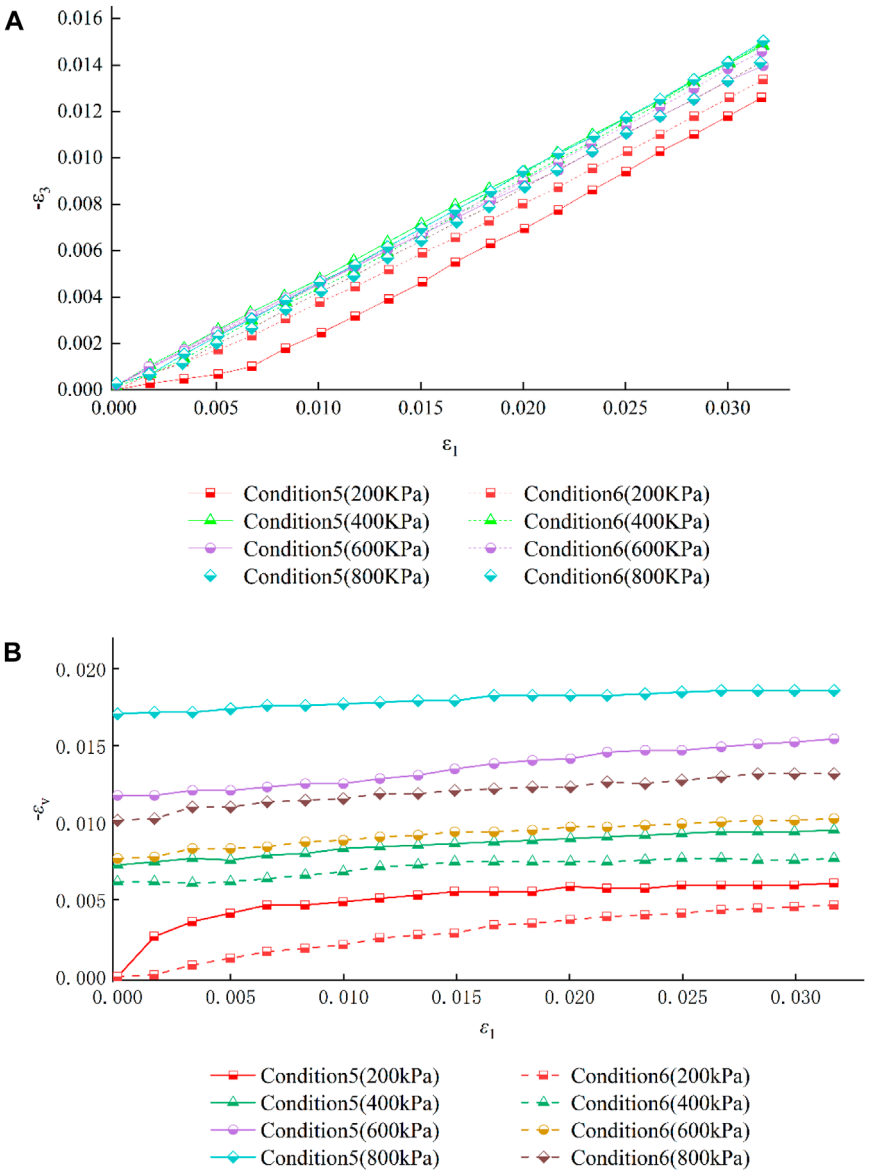

FIGURE 9
Curves of strain relationship. **(A)** Curves of the relationship between lateral strain and axial strain. **(B)** Curves of the relationship between volumetric strain and axial strain.

3.3 Deformation characteristics analysis

In this test, Condition 6 is a 2-layer reinforced, 20-cm spacing large-scale triaxial gravelly soil CD test, and Condition 5 is a large-scale triaxial CD test of unreinforced gravelly soil under the same conditions. Figure 9A shows the lateral strain and axial strain curves of the relationship between the samples in Conditions 5 and 6 under different confining pressures.

Figure 9A shows that the lateral deformation of the reinforced gravelly soil is smaller than that of the unreinforced gravelly soil at the same axial strain under high confining pressures, and the difference is small. Under low confining pressures, the lateral deformation of reinforced gravelly soils is larger than that of unreinforced gravelly soils, and the difference is larger.

Figure 9B shows the volumetric strain and axial strain curves of the samples in working conditions 5 and 6 under different confining pressures. Figure 9B shows that the variations in volumetric strain of unreinforced and reinforced gravelly soils at higher confining pressures are smaller than those in the volumetric strain rate at lower confining pressures. The volumetric strain in reinforced gravelly soils is smaller than that in unreinforced gravelly soils at the same confining pressure and the same axial strain. The higher the confining pressure is, the greater the difference between the reinforced and unreinforced volumetric strains. At the same confining pressure, the shear expansion of unreinforced samples is more obvious than that of reinforced samples.

TABLE 5 The difference of main stress when the gravelly soils triaxial test under different reinforced layers damages.

Conditions	Reinforcement layers	Confining pressure (MPa)			
		200	400	600	800
Condition1	—	0.87	1.82	2.57	3.50
Condition2	1	1.02	2.01	2.82	3.70
Condition3	2	1.13	2.14	3.03	3.83
Condition4	3	0.96	2.00	2.94	3.82

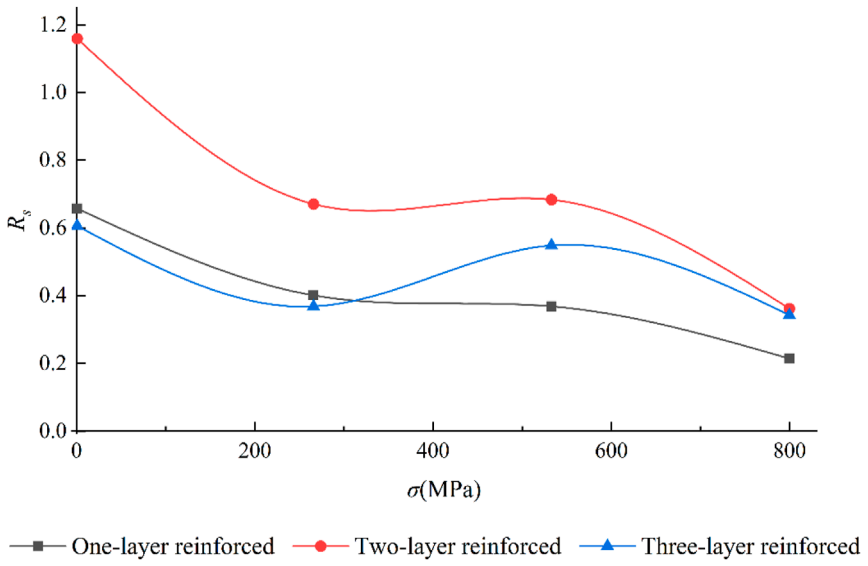

FIGURE 10
Reinforced soil strength and coefficient of gravelly soil.

4 Discussions

The reinforcement effect of geogrid-gravelly soil was analyzed based on the results of triaxial test. From the stress-strain curves of unreinforced gravelly soils and reinforced gravelly soils, it can be seen that there is no peak in the principal stress difference, and the principal stress difference at 15% is taken as the failure principal stress difference, as shown in Table 5.

To evaluate the reinforcing effect of the geogrid on gravelly soil, the geogrid reinforcement coefficient R_s was introduced. Chen et al. (2014) referred to the ratio of the critical shear strength of reinforced and unreinforced soil under the same confining pressure as the geogrid reinforcement coefficient R_s of the geogrid to evaluate the reinforcing effect of the geosynthetic material:

$$Rs = \frac{(\sigma_1 - \sigma_3)_f^R}{(\sigma_1 - \sigma_3)_f} \quad (1)$$

$(\sigma_1 - \sigma_3)_f^R$ and $(\sigma_1 - \sigma_3)_f$ in Eq. 1 are the critical shear strengths of the geogrid-reinforced and unreinforced gravelly soil samples, respectively. The σ_3–R_S curves for different numbers of reinforcement layers are shown in Figure 10.

Under a high confining pressure, the geogrid reinforcement coefficient is smaller, mainly because the high confining pressure causes the lateral deformation to be small and the lateral restraint capacity of the geogrid cannot be fully developed. At a low confining pressure, the lateral deformation is large, and the tensile stress of the geogrid comes into play only when the strain accumulates to a certain amount, hence increasing the shear strength of reinforced gravelly soils (Chen et al., 2014). This conclusion indicates that the geogrid reinforcement materials in the soil can exert their reinforcing effect only when a certain deformation of the soil occurs. Figure 10 shows that the reinforcement effect differs under different confining pressure and axial strain conditions. In the triaxial tests, we find that the reinforcement effect of 2 layers under 200–400 MPa confining pressure is better than those of 1 layer and 3 layers, and the reinforcement effects of 1 layer and 3 layers are similar other; the reinforcement effect of 2 layers under 400–800 MPa confining pressure is also better than those of 1 layer and 3 layers, and the reinforcement effect of 3 layers is better than that of 1 layer. The reason for this is that the 1st and 3rd reinforcement layers of the 3-layer reinforced sample are too close to the top and bottom of the sample, resulting in the sample being affected by the end

boundary effect, which makes the lateral deformation of the end of the sample smaller. The geogrid deformation is small enough that it does not truly reflect the reinforcement effect of the geogrid (Wang-Guo et al., 2010).

The analysis shows that the geogrid reinforcement coefficient Rs is greater than 1. In the range of 200–800 MPa confining pressure, Rs is typically between 1.06 and 1.30. According to other scholars' research results, geogrid reinforcement coefficients are greater at low confining pressure (Jiang et al., 2018), indicating that reinforcement can significantly improve the shear strength of gravelly soils.

5 Conclusion

This study discusses large-scale triaxial tests on three typical gravelly soils (round gravelly soil, angular gravelly soil, and sandy soil) in Xinjiang without geogrids or with different spacings of geogrids using a large-scale static and dynamic triaxial instrument. The shear strength, deformation characteristics, and internal friction angle of gravelly soils with different particle shapes, as well as the stress–strain relationships, strength characteristics, failure modes, and reinforcement effects of gravelly soils with and without reinforcement, are compared and analyzed. The main conclusions are as follows.

(1) When a geogrid with an elastic modulus much larger than that of gravelly soil is used to form a geogrid-gravelly soil composite, an inward friction resistance is generated between the reinforcement and soil, which increases the surrounding pressure and effectively improves the soil strength. However, only when the soil has a certain deformation or the soil and reinforcement material have a certain relative displacement can the reinforcement produce a certain restraining effect on the soil and provide the effect of reinforcement.

(2) The three types of unreinforced gravelly soils in the unsaturated state have a nonzero cohesion c. The geogrid-reinforced gravelly soils conform to the Mohr-Coulomb shear strength failure criterion, and the reinforcement mechanism can be explained by pseudo-cohesion theory, i.e., the equivalent confining pressure increment $\Delta\sigma_3$ of the reinforced composite is essentially the same as the cohesion increment Δc. The effect of reinforcement on the φ of the gravelly soils is small, and the φ values are basically unchanged with and without reinforcement. The cohesion c increases significantly with reinforcement, indicating that the reinforcement can obviously improve the shear strength of these gravelly soils.

(3) The reinforcement coefficient R_s with reinforcement increases significantly with the number of reinforcement layers, but the higher the confining pressure of the triaxial samples is, the smaller the reinforcement coefficient.

(4) Reinforcement inhibits the lateral expansion of the reinforced specimens, resulting in a substantial increase in shear strength and a reduction in volumetric strain. Under the same triaxial test conditions, the volumetric strain of the gravelly soil samples decreases markedly with reinforcement, and the higher the confining pressure is, the larger the volumetric strain between reinforcement conditions. The shear dilation phenomenon of unreinforced samples is more obvious than that of reinforced samples, and the samples are shown to be of the strain-hardening type with and without reinforcement.

Data availability statement

The original contributions presented in the study are included in the article/Supplementary material, further inquiries can be directed to the corresponding author.

Author contributions

JL: Data curation, Writing–original draft. JP: Data curation, Writing–original draft. BW: Writing–review and editing. CH: Writing–review and editing. QL: Writing–review and editing.

Funding

The author(s) declare financial support was received for the research, authorship, and/or publication of this article. This study was funded by the enterprise commissioned science and technology project of Xinjiang Traffic Design Institute Company (No. KY2022121902). The funder was not involved in the study design, collection, analysis, interpretation of data, the writing of this article or the decision to submit it for publication.

Conflict of interest

Authors JiL, JP, BW, CH, and QL were employed by Xinjiang Transport Planning Survey and Design Institute Co., Ltd.

Publisher's note

References

Ai, X., Wang, G., Kong, X., Cui, B., Hu, B., and Ma, H. (2021). The scale effect of coarse-grained materials by triaxial test simulation. *Adv. Civ. Eng.* 2021, 1–13. doi:10.1155/2021/6665531

Asakereh, A., Ghazavi, M., and Tafreshi, S. M. (2013). Cyclic response of footing on geogrid-reinforced sand with void. *Soils Found.* 53 (3), 363–374. doi:10.1016/j.sandf.2013.02.008

Berre, T. (1986). Suggested international procedure for triaxial compression tests. *Submitt. ISSMFE Subcomm. Soil Test. Also NGI Intern. Rep.*, 56103–56130.

Chen, X., Jia, Y., and Zhang, J. (2018). Stress-strain response and dilation of geogrid-reinforced coarse-grained soils in large-scale direct shear tests. *Geotechnical Test. J.* 41 (3), 20160089. doi:10.1520/GTJ20160089

Chen, X., Zhang, J., and Li, Z. (2014). Shear behaviour of a geogrid-reinforced coarse-grained soil based on large-scale triaxial tests. *Geotext. Geomembranes* 42 (4), 312–328. doi:10.1016/j.geotexmem.2014.05.004

Du, C., Niu, B., Wang, L., Yi, F., and Liang, L. (2022). Experimental study of reasonable mesh size of geogrid reinforced tailings. *Sci. Rep.* 12 (1), 10037. doi:10.1038/s41598-022-13980-x

Estabragh, A., Bordbar, A., and Javadi, A. (2011). Mechanical behavior of a clay soil reinforced with nylon fibers. *Geotechnical Geol. Eng.* 29, 899–908. doi:10.1007/s10706-011-9427-8

Gu, F., Luo, X., Luo, R., Lytton, R. L., Hajj, E. Y., and Siddharthan, R. V. (2016). Numerical modeling of geogrid-reinforced flexible pavement and corresponding validation using large-scale tank test. *Constr. Build. Mater.* 122, 214–230. doi:10.1016/j.conbuildmat.2016.06.081

Guo, C. C. (2003). Discussion of triaxial shear test for multilevel adding load of a kind of samples. *Electr. Power Surv*. doi:10.3969/j.issn.1671-9913.2003.01.008

Hai-tao, L., and Xiao-hui, C. (2009). Discrete element analysis for size effects of coarse-grained soils. *Rock Soil Mech.* 30, 287–292. doi:10.3969/j.issn.1000-7598.2009.z1.057

Huachen, C. (2004). Study on applicability of multilevel loading triaxial compression test to a sample. *site investigation Sci. Technol.* doi:10.3969/j.issn.1001-3946.2004.04.010

Jia-ming, Z., Guo-sheng, J., and Ren, W. (2009). Research on influences of particle breakage and dilatancy on shear strength of calcareous sands. *Rock Soil Mech.* 30 (7), 2043–2048. doi:10.3969/j.issn.1000-7598.2009.07.029

Jiang, J.-Q., Yang, G.-L., Li, L.-M., and He, G.-W. (2018). Experimental investigation on mechanical behavior of a hexagonal-wire-reinforced granular soil. *Arabian J. Sci. Eng.* 43, 1655–1672. doi:10.1007/s13369-017-2668-y

Koga, K., Aramaki, G., and Valliappan, S. (1988). "Finite element analysis of grid reinforcement," in *International geotechnical symposium on theory and practice of earth reinforcement*, 407–411.

Liu, F., and Cai, Y. (2009). "Dynamic finite element analysis of reinforced and unreinforced pavements over soft clay," in *Geosynthetics in civil and environmental engineering: geosynthetics asia 2008 proceedings of the 4th asian regional conference on geosynthetics in shanghai* (China: Springer), 683–687.

Liu, W. B., and Chen, Z. Y. (2011). Study of the deformation field of reinforced soil on the triaxial text. *Appl. Mech. Mater.* 71, 5024–5029. doi:10.4028/www.scientific.net/AMM.71-78.5024

Mittal, A., and Shrivastava, A. K. (2020). Stress–strain characteristics of landfill clay cover barriers under geogrid reinforcements. *Innov. Infrastruct. Solutions* 5, 19–9. doi:10.1007/s41062-020-0263-7

Qingguo, G. (1999). *Properties of the coarse grained soils and its application*. Beijing: Yellow River Press, 36–39.

Qu, J., and Sun, Z. (2016). Strength behavior of shanghai clayey soil reinforced with wheat straw fibers. *Geotechnical Geol. Eng.* 34, 515–527. doi:10.1007/s10706-015-9963-8

Ruan, B., Zheng, S., Teng, J., Ding, H., and Ma, C. (2020). Analysis on the triaxial shear behavior and microstructure of cement-stabilized clay reinforced with glass fibers. *Adv. Civ. Eng.* 2020, 1–12. doi:10.1155/2020/8842091

Sarkar, S., and Hegde, A. (2022). "Strength enhancement of geogrid reinforced marginal backfill materials in triaxial condition," in *Geo-congress 2022*, 467–476.

Shengyou, L. (2006). *Theory and technology of modern reinforced soil*. Beijing: China Communication Press, 75–81.

Skuodis, Š., Dirgėlienė, N., and Medzvieckas, J. (2020). Using triaxial tests to determine the shearing strength of geogrid-reinforced sand. *Studia Geotechnica Mech.* 42 (4), 341–354. doi:10.2478/sgem-2020-0005

Tang, K., Xie, X., and Yang, L. (2014). Research on mechanical characteristics of gravel soil based on large-scale triaxial tests. *Chin. J. Under Space Eng.* 10, 580–585.

Tong, F., Ma, Q., and Xing, W. (2019). Improvement of clayey soils by combined bamboo strip and flax fiber reinforcement. *Adv. Civ. Eng.* 2019, 1–10. doi:10.1155/2019/7274161

Wang, Q., Wen, X., Jiang, J., Zhang, C., and Shi, Z. (2014). Experimental study on performance of multidirectional geogrid and its application in engineering of high slope. *J. Wuhan Univ. Technology-Mater. Sci. Ed.* 29 (4), 704–711. doi:10.1007/s11595-014-0984-6

Wang-Guo, X., Jia-Sheng, Z., and Jianqing, H. (2010). Research on large-scale triaxial tests on reinforced soft rock composed of coarse-grained soil as embankment fillings. *Chin. J. Rock Mech. Eng.* 29 (3), 535–541.

Yang, B., Chen, Y., Zhao, C., and Li, Z. (2023). Effect of geotextiles with different masses per unit area on water loss and cracking under bottom water loss soil conditions. *Geotext. Geomembranes* 52, 233–240. doi:10.1016/j.geotexmem.2023.10.006

Ye, F., and Fu, W. (2018). Physical and mechanical characterization of fresh bamboo for infrastructure projects. *J. Mater. Civ. Eng.* 30 (2), 05017004. doi:10.1061/(ASCE)MT.1943-5533.0002132

Yi, P. Y. (2011). The stress variation and mechanism of bearing capacity increment in reinforced foundation. *Appl. Mech. Mater.* 71, 3769–3774. doi:10.4028/www.scientific.net/AMM.71-78.3769

Yong-zhen, Z., Wei, Z., Jia-jun, P., and Na, Z. (2015). Effects of gradation scale method on maximum dry density of coarse-grained soil. *Rock Soil Mech.* 36, 417–422.

Yu, Z., Woodward, P., Laghrouche, O., and Connolly, D. P. (2019). True triaxial testing of geogrid for high speed railways. *Transp. Geotech.* 20, 100247. doi:10.1016/j.trgeo.2019.100247

Zekkos, D., Bray, J. D., and Riemer, M. F. (2008). Shear modulus and material damping of municipal solid waste based on large-scale cyclic triaxial testing. *Can. Geotechnical J.* 45 (1), 45–58. doi:10.1139/t07-069

Zekkos, D., Bray, J. D., and Riemer, M. F. (2012). Drained response of municipal solid waste in large-scale triaxial shear testing. *Waste Manag.* 32 (10), 1873–1885. doi:10.1016/j.wasman.2012.05.004

Zhang, H.-Q., Zhao, F., Cheng, S.-Q., Zhang, Y.-Q., Gou, M.-J., Jing, H.-J., et al. (2020). Study of sericite quartz schist coarse-grained soil by large-scale triaxial shear tests. *Front. Phys.* 8, 551232. doi:10.3389/fphy.2020.551232

Zhang, Z., Ji, E., and Fu, Z. (2022). Study on the tensile properties and application of gravelly soil reinforced by polypropylene fiber. *KSCE J. Civ. Eng.* 26 (8), 3265–3274. doi:10.1007/s12205-022-0923-6